

# Preparation and Characterization of Copper Telluride Thin Films

Remant Morbaita<sup>1</sup>, A.L. Yadav<sup>2</sup>, and Suresh Kumar Sahani<sup>\*3</sup>

<sup>1</sup> RRM Campus, Janakpurdham, TU, Nepal remantmorbaita108@gmail.com

<sup>2</sup> DS Campus, Janakpurdham, Nepal alyphy@gmail.com

<sup>\*3</sup> Department of Science and Technology, Rajarshi Janak University,  
Janakpurdham, Nepal sureshsahani@rju.edu.np

## Abstract

Copper telluride thin films were deposited using a modified chemical technique with copper(II) sulphate pentahydrate [CuSO<sub>4</sub>·5H<sub>2</sub>O] and sodium tellurite [Na<sub>2</sub>TeO<sub>3</sub>] as cationic and anionic sources, respectively. The modified chemical technique is based on immersing the substrate in distinct cationic and anionic precursors. The preparative parameters, such as concentration, pH, immersion time, immersion cycles, and so on, were tuned to produce high-quality copper telluride thin films at room temperature. X-ray diffraction (XRD), scanning electron microscopy (SEM), and energy dispersive X-ray analysis (EDAX) were used to study the films' structural, compositional, optical, and electrical transport properties.

**Keywords:** Cupric telluride, thin film, sodium tellurite, cationic, XRD, EDAX, SEM.

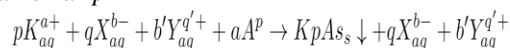
## 1 Introduction

Because of their vast range of applications in numerous domains of science and technology, semi-conducting copper chalcogenide thin films have sparked increased attention in recent decades. Copper chalcogenide thin films are used in a variety of devices, including solar cells, super ionic conductors, photodetectors, photothermal conversion, electroconductive electrodes, microwave shielding coatings, and so on. Copper telluride is a copper chalcogenide (compound from groups I-VI). Depending on the value of  $x$  ( $1 < x < 2$ ), copper telluride (Cu<sub>2</sub>Te) has distinct crystal forms (see[1-15]). The optical band gap of Cu<sub>2</sub>Te is  $\approx 1.1$  eV.

Thin film deposition by a modified chemical approach has recently piqued the interest of researchers since it offers numerous advantages over the more recognized synthetic route to semiconductor materials. Controlling film thickness and deposition rate by adjusting pH, reagent concentration, and complexing agent are combined with the ability to coat a vast surface at a reasonable cost. The modified chemical approach can be employed for aqueous solution deposition at room temperature. The growth mode is the primary distinction between chemical bath deposition (CBD) and modified chemical methods. In CBD, all of the

precursors are present in the reaction vessel at the same time, but in the modified chemical technique, each precursor is treated separately on the substrate, and rinse separates these treatments. As the separate stages are isolated by washing, the adsorbed species on the substrate surface govern the reactions and film formation occurs. The number of deposition cycles directly controls the thickness of the layers(see[16-35]).

The modified chemical approach is based on a sequential reaction at the surface of the substrate. Each reaction is followed by rinsing, which allows for heterogeneous interaction between the solid phase and the solvated ions in the solution. The goal is to produce thin films of water-insoluble ionic or ion covalent compounds of the KpAa type by a heterogeneous chemical reaction at the solid solution interface between adsorbed cations  $pK^{a+}$  and anion  $aAp^{-}$



with  $ap = bq = b'q$ . Where K represents the cation (Cd<sup>2+</sup>, Zn<sup>2+</sup>, Fe<sup>3+</sup>, Cu<sup>+</sup>, etc.), p the number of cations, a the numerical value of charge on cation, X an ion in cationic precursors having negative charge ( $X = SO_4^{2-}$ , Cl<sup>-</sup>, NO<sub>3</sub><sup>-</sup> etc.), q the number of X in cationic precursors, b the numerical value of charges on X,

b' the number of Y in the anionic solutions, q' the numerical value of charge on Y, Y the ion which is attached to chalcogen ion, A the anion (O, S, Se and Te) and a the number of anions.

A number of attempts have been made to deposit  $\text{Cu}_x\text{S}$  and  $\text{Cu}_x\text{Se}$  thin films using a modified CBD technique; however, no report on the deposition of copper telluride thin films is published. In this study, semi-conducting copper telluride thin films were formed onto glass substrates at room temperature using a modified chemical technique. X-ray diffraction (XRD), scanning electron microscopy (SEM), energy dispersive X-ray analysis (EDAX), Rutherford back scattering (RBS), optical absorption, electrical resistivity, and thermoelectric measurements were used to characterize the films' structural, surface morphological, compositional, optical, and electrical properties (see [36-51]).

## 2 Experimental

### 2.1 Copper telluride thin film formation

The deposition was carried out on  $75 \text{ mm} \times 25 \text{ mm} \times 1 \text{ mm}$  commercially available glass microslides.

	Precursor	$\text{CuSO}_4(2 \text{ NTEA}^a + 2 \text{ NHH}^b)$	$\text{Na}_2\text{TeO}_3$
1	Concentration(M)	0.1	0.05
2	pH	5	9
3	Immersion time(s)	20	20
4	Number of immersions	60	60
5	Deposition temperature (K)	300	300

Table 1: Conditions for deposition of copper telluride thin films using a modified chemical technique.

### 2.2 Characterization of the copper telluride thin films

The weight difference approach was used to determine the thickness of the copper telluride layer. The X-ray diffraction pattern of copper telluride films was obtained using a Philips model PW 1710 in the scanning angle range of  $20-60^\circ (2\theta)$  with  $\text{CuK}\alpha$  radiations at  $1.5418 \text{ \AA}$ . The copper telluride thin film's microstructure and chemical composition were determined using scanning electron microscopy and energy dispersive X-ray analysis on a Philips XL-30 SEM and an EDAX analyzer, respectively.  $1.8 \text{ MeV He}^+$  ions were used in the Rutherford back scattering study of films on glass substrate. The ion beam was incident on the surface

The microslides were boiled in chromic acid for 30 minutes before being washed with detergent, rinsed with acetone, and ultrasonically cleaned with double distilled water. The following process was used to deposit copper telluride films from an aqueous solution: Copper telluride's cationic precursor was  $0.1 \text{ M}$  copper sulphate pentahydrate  $[\text{CuSO}_4 \cdot 5\text{H}_2\text{O}]$  at a pH of 5. The telluride ion was obtained from  $0.05 \text{ M}$  sodium tellurite with a pH of 9. For 20 seconds, a clean glass substrate was immersed in a copper sulphate solution, where copper ions were adsorbed on the surface of the glass substrate. To remove weakly bound or excess copper ions from the glass substrate, it was washed in deionized water for 50 seconds. The glass substrate was then immersed for 20 seconds in an anionic precursor ( $\text{Na}_2\text{TeO}_3$ ) solution, where telluride ions reacted with pre-adsorbed copper ions on the glass substrate to generate a copper telluride layer on the glass's surface. The optimum deposition conditions for copper telluride are listed in table 1. a TEA: triethanolamine. b HH: hydrazine hydrate.

of the film, and a semiconductor detector (implanted Si detector, solid angle of  $3.4 \times 10^{-3} \text{ sr}$ ) was installed at a scattering angle of  $170^\circ$ . The energy resolution exceeded  $20 \text{ keV}$ . To achieve a statistical error of 1%, about  $(1-3) \times 10^5$  counts per peak were sampled. The composition of the film can be established by recreating the films' Rutherford back scattering spectra with software and fitting them to experimental data. To investigate the optical characteristics, optical absorption and transmission were measured using a Hitachi 330 spectrophotometer in the wavelength range of  $350-850 \text{ nm}$ . The electrical resistivity of the film was measured in the temperature range of  $300-500 \text{ K}$  using a dc two-point probe method. The temperature

difference was measured using a chromel alumel thermocouple and a brass block as a sample holder. The polarity of the thermally generated voltage at the hot end of the lm was used to determine the type of electrical conductivity of the lm.

### 3 Results and discussion

#### 3.1 Thickness measurement

Thickness of the copper telluride lms for different number of deposition cycles was measured using weight difference method given by

$$1) \quad t = \frac{m}{A\rho}$$

where  $m$  is the mass of the lm,  $A$  is the area of the lm and  $\rho$  ( $7.303 \text{ g/cm}^3$ ) the mean density ( $\text{Cu}_2\text{Te}$ :  $7.27 \text{ g/cm}^3$ ;  $\text{CuTe}$ :  $7.10 \text{ g/cm}^3$ ;  $\text{Cu}_{1.4}\text{Te}$ :  $7.54 \text{ g/cm}^3$  of deposited material, as discussed in Section 3.2. The change of copper telluride lm thickness for the number of deposition cycles with optimum deposition circumstances is shown in Fig. 1. For 50 deposition cycles, a final thickness of  $0.36 \text{ }\mu\text{m}$  was discovered. The rate of growth was determined to be  $7.2 \text{ nm}$  per cycle.

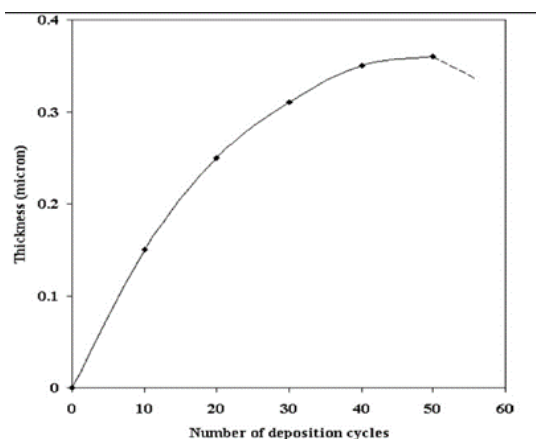


Figure 1: Thickness vs deposition cycle count for copper telluride thin lm.

The lms got powdery and aaked o the glass substrate after 50 cycles. Previously, similar behavior was observed in  $\text{Bi}_2\text{S}_3$  thin lms created by modified chemical bath deposition (M-CBD).

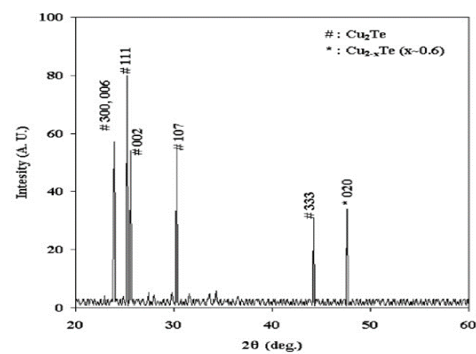


Figure 2: XRD pattern of copper telluride thin lm placed on glass substrate.

	Observed 'd'	Standard 'd'	Plane hkl	Phase
1	3.61	3.61	3 0 0, 0 0 6	$\text{Cu}_2\text{Te}$
2	3.52	3.51	1 1 1	$\text{Cu}_2\text{Te}$
3	3.47	3.47	0 0 2	$\text{CuTe}$
4	2.94	2.99	1 0 7	$\text{Cu}_2\text{Te}$
5	2.04	2.04	0 2 0	$\text{CuTe}$
6	1.91	1.939	0 2 0	$\text{Cu}_{2-x}\text{Te}$
7	1.51	1.52	1 0 4	$\text{Cu}_2\text{Te}$

Table 2: Composition of XRD and ASTM data from copper telluride thin lms formed using a modified chemical technique.

#### 3.2 Structural studies

Fig. 2 depicts the XRD pattern of a copper telluride lm on a glass substrate. Table 2 compares observed interplaner distance 'd' values to standard 'd' values from ASTM data. The deposited material is copper telluride with mixed cubic and tetragonal crystal structure [mixed phases of  $\text{Cu}_2\text{Te}$ ,  $\text{CuTe}$ , and  $\text{Cu}_{2-x}\text{Te}$ ] based on a comparison of measured 'd' values with standard 'd' values.

No further phases of Cu and Te were found in the XRD pattern, which could be owing to the amorphous structure or a low fraction of the same.

#### 3.3 Scanning electron microscopy (SEM) and energy dispersive Xray analysis (EDAX)

SEM is a handy technique for studying the surface microstructure of thin lms. Scanning electron micrographs of copper telluride thin lms produced on glass substrates at 1000 and 10,000 magnifications are shown in Figs. 3a and b. According to Fig. 3, the copper telluride thin lm is uniform, smooth, and homogeneous, and it is well covered to the substrate. Fine-grained surface

particles of copper telluride lm are seen in Fig. 5.3b. Copper telluride thin lm on glass substrate was analyzed using energy dispersive X-rays. According to the results of the investigations, the average at % composition of the lm is Cu:Te 67 : 33.

### 3.4 Rutherford back scattering

The Rutherford back scattering spectrum of a copper telluride lm on a glass substrate is shown in Fig. 4. It plots the number of detected back-scattered He ions as a function of their energy alongside simulated copper telluride spectra. The solid curve depicts the computed RBS spectra of Cu Te on glass. Cu and Te were considered to be homogeneously distributed in thin lm for calculation purposes. The presence of oxygen is also indicated by a tiny peak with an edge energy of 650 keV. The presence of oxygen and Si peaks in RBS spectra is due to the substrate's amorphous glass ( $\text{SiO}_2$ ). The presence of oxygen has been discovered in numerous chemically formed lms using the RBS approach. The integrated counts under curves (peak and tail) coincide with the counts under simulated peaks, showing that the lm is Cu Te.

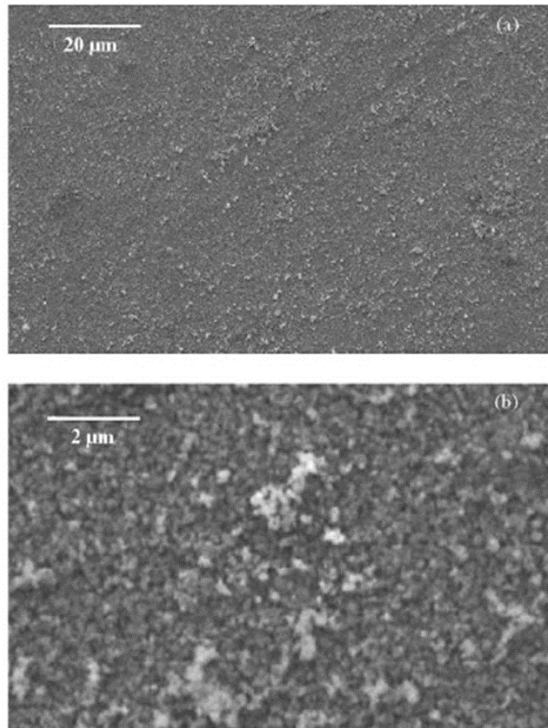


Figure 3: Scanning electron microscopy (SEM) of copper telluride thin lm at (a) 1000X and (b) 10,000X magnifications.

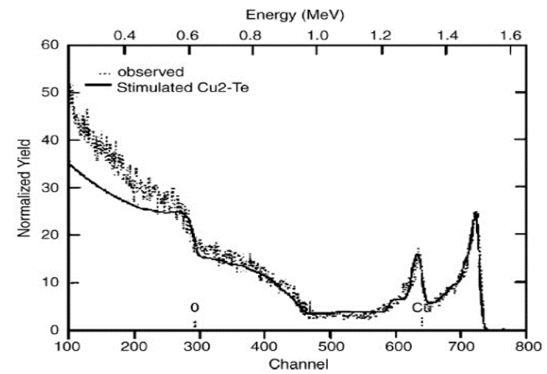


Figure 4: Spectra of RBS for a copper telluride thin lm on a glass substrate.

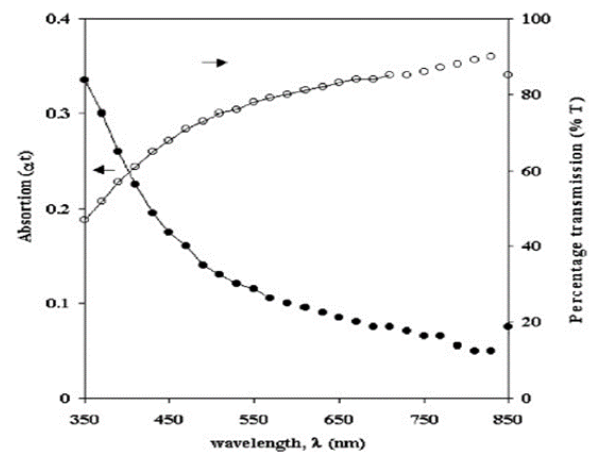


Figure 5: Absorption (at) and transmittance (T %) plots against wavelength ( $\lambda$ ) for copper telluride thin lm.

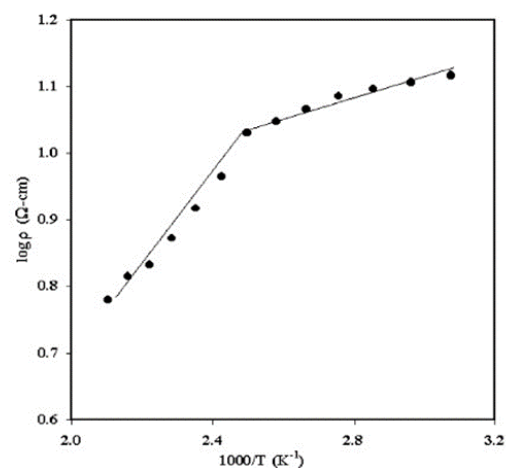


Figure 6: The plot of  $\log \rho$  versus  $1000/T$  for thin lm of copper telluride.

### 3.5 Optical studies

The optical absorption and transmission spectra [Fig.5] of a copper telluride thin film coated on a glass substrate (thickness  $\sim 0.2$  mm) were measured using a spectrophotometer (Hitachi Model 330) in the wavelength range 350–850 nm. According to these spectra, the film shows a high absorbance ( $10^4 \text{ cm}^{-1}$ ) indicating a direct band gap transition. However, the maximum percentage transmission (90%) occurs at  $\lambda = 830$  nm.

### 3.6 Electrical resistivity and thermoelectric measurement

A dc two-point probe approach was used to test the dark electrical resistivity ( $\rho$ ) of the copper telluride film. Figure 6 depicts the variance of  $\log \rho$  versus  $1000/T$  for the film. The resistance reduces with increasing temperature, showing that the copper telluride coating is semi-conducting. At room temperature, the dark electrical resistivity was on the order of  $10^1 \Omega \cdot \text{cm}$ , which is the same as the value ( $10^1 \Omega \cdot \text{cm}$ ) reported previously for electrodeposited  $\text{Cu}_x\text{Te}$  thin films. The variation is also shown to be non-linear. The graph is divided into two sections that correlate to low and high temperatures. Similar results have already been reported for copper sulphide thin films. The temperature dependency drives carrier transfer from the hot to cold end, giving birth to the thermal voltage. Thermoelectric voltage was measured for copper telluride thin films at temperatures ranging from 300–500 K. The thermally generated voltage at the hot end had a negative polarity, indicating that the material is p-type. The rise in thermoelectric voltage with temperature difference could be due to an increase in the mobility of charge carriers as temperature difference rises.

## 4 Conclusions

A modified chemical approach can be used to generate copper telluride thin films on glass substrates.

The film is made up of various phases of copper telluride ( $\text{CuTe}$ ,  $\text{Cu}_2\text{Te}$ , and  $\text{Cu}_{2-x}\text{Te}$ ). The absence of  $\text{Cu}_2\text{O}$ ,  $\text{TeO}_2$ , and other oxides observed may be attributable to their amorphous nature or a low fraction of them. The electrical resistivity at room temperature was measured to be on the order of  $10^1$

$\Omega \cdot \text{cm}$ .  $\text{Cu}_x\text{Te}$  films deposited with M-CBD exhibit p-type electrical conductivity.

## 5 Acknowledgment

We would like to express our heartfelt gratitude to all those who have contributed to the successful completion of this research report.

## References

- [1] Milton Ohring. The Material Science of Thin Films. Academic Press New York, 1992.
- [2] K. Wasa, M. Kitabatake, and H. Adachi. Thin Film Material Technology. Springer, 2004.
- [3] B. Lio, Y. Xie, J. Huang, Y. Liu, and Y. Qian. Chem. Mater., 12:2614, 2000.
- [4] H. Saloniemi, T. Kanninen, M. Ritala and M. Leskela: Thin Solid Films 326 (1998) 78–82.
- [5] R. Chen, D. Xu, G. Guo and L. Gui: J. Mater. Chem. 12 (2002) 2435–2438.
- [6] J. W. Gardner: Engl. Electr. J. 18 (1963) 16–21.
- [7] W. Lehmann: J. Electrochem. Soc. 104 (1957) 45–50.
- [8] D. A. Cusano: Solid State Electron. 6 (1963) 217–232.
- [9] M. Aven and D. A. Cusano: J. Appl. Phys. 35 (1964) 606–611.
- [10] P. J. Mosticak: Phys. Status Solidi. 11 (1972) 531–538.
- [11] G. P. Sorokin, G. Z. Idrichan, L. V. Derkach, E. V. Kovton and Z. M. Sorokina: Izv. Akad. Nauk S. S. S. R. Neorg. Mater. 10 (1974) 969–974.
- [12] K. Srudhar and K. Chattopadhyay: J. Alloys Compd. 264 (1998) 293–299.
- [13] Allen J. Bard and Larry R. Faulkner: Electrochemical Methods, (John Wiley and Sons, Inc, United States of America, 1980) p. 32.
- [14] I. Barin: Thermochemical Data of Pure Substances Part II, (VCH, 1989).
- [15] M. Pourbaix: Atlas of Electrochemical Equilibria in Aqueous Solution, (Pergamon Press, Oxford, 1966) p. 385.
- [16] R. K. Pandey and S. N. Chandra: Handbook of Semiconductor Electrodeposition, (Marcel Dekker, Inc, New York, 1996) p. 44.
- [17] JCPDS Data Base, Card No. 39-1061 (unindexed peaks), JCPDS, Swarthmore, PA. JCPDS Data Base, Card No. 39-1061 (unindexed peaks), JCPDS, Swarthmore, PA.

- [18] W. S. Chen, J. M. Stewart, R. A. Mickelsen, *Appl. Phys. Lett.* 46, 1095 (1985).
- [19] C. Nascu, I. Pop, V. Ionscu, E. Indra, I. Bratu, *Mater. Lett.* 32, 73 (1997). [20] H. Okimura, T. Matsumae, R. Makabe, *Thin Solid Films* 71, 53 (1980).
- [21] M. A. Korzhuev, *Phys. Solid State* 40, 217 (1998).
- [22] H. M. Pathan, C. D. Lokhande, D. P. Amalnerkar T. Seth. *Appl. Surf. Sci.* 218, 290 (2003).
- [23] P. F. Carcia, F. D. Kalk, P. E. Bierstedt, A. Feretti, G. A. Jones, D. G. Swartzfager, *J. Appl. Phys.* 64, 1671 (1988).
- [24] C. Paparoditis, C. Stella, D. Darmagna, J. Bernard, (*Comm. Coll. Int. Phys. Couches Minces, Clausthal, Gottingen*) 732 (1965).
- [25] Gurevich, S. B. and V. B. Konstantinov, "Real-time holographic interferometry in a physical experiment," *J. Opt. Technol.*, Vol. 63, No. 10, 725, 1996.
- [26] Pawar, S. J., P. P. Chikode, V. J. Fulari, and M. B. Dongare, "Studies on electrodeposited silver selenide thin film by double exposure holographic interferometry," *Mater. Sci. Eng. B*, Vol. 137, 232, 2007.
- [27] Chen, W. S., J. M. Stewart, and R. A. Mickelsen, "Chemical deposition and characterization of  $\text{Cu}_3\text{Se}_2$  and  $\text{CuSe}$  thin films," *Appl. Phys. Lett.*, Vol. 46, 1095, 1985.
- [28] Neyvasagam, K., N. Soundararajan, Ajaysoni, G. S. Okram, and V. Ganesan, "Low-temperature electrical resistivity of cupric telluride ( $\text{CuTe}$ ) thin films," *Physica Status Solidi (b)*, Vol. 245, 77, 2007.
- [29] Okimura, H., T. Matsumae, and R. Makabe, "Electrical properties of  $\text{Cu}_2\text{xSe}$  thin films and their application for solar cells," *Thin Solid Films*, Vol. 71, 53, 1980.
- [30] Korzhuev, M. A., "Dufour effect in superionic copper selenide," *Phys. Solid State*, Vol. 40, 217, 1998.
- [31] Fonash, S. J., *Solar Cells Device Physics*, 78, Academic Press, San Diego, 1981.
- [32] Pathan, H. M. and C. D. Lokhande, "Deposition of metal chalcogenide thin films by successive ionic layer absorption and reaction (SILAR) method," *Bull. Mater. Sci.*, Vol. 27, 85, 2004.
- [33] Collier, R. J., C. B. Burckhardt, and L. H. Lin, *Optical Holography*, Academic, New York, 1971.
- [34] Prabhune, V. B., N. S. Shinde, and V. J. Fulari, "Studies on electrodeposited silver sulphide thin films by double exposure holographic interferometry," *Appl. Surf. Sci.*, Vol. 255, 1819, 2008.
- [35] Chikode, P. P., S. J. Pawar, V. J. Fulari, and M. B. Dongare, "Study of diffusion process in sucrose solution by using double exposure holographic interferometry (DEHI)," *J. Opt.*, Vol. 36, 157, 2007.
- [36] Dongare, M. B., V. J. Fulari, and H. R. Kulkarni, "Monitoring the deposition of Cu thin film using the double exposure holographic interferometry technique," *Thin Solid Films*, Vol. 301, 62, 1997.
- [37] Pawar, S. J., P. P. Chikode, V. J. Fulari, and M. B. Dongare, "Studies on electrodeposited silver selenide thin film by double exposure holographic interferometry," *Material Science and Engineering*, Vol. B37, 232, 2007.
- [38] JCPDS data file No. 22-0252.
- [39] Pathan, H. M., C. D. Lokhande, D. P. Amalnerkar, and T. Seth, "Preparation and characterization of copper telluride thin films by modified chemical bath deposition (M-CBD) method," *Applied Surface Science*, Vol. 218, 290, 2003.
- [40] Mane, R. S., S. J. Roh, O.-S. Joo, C. D. Lokhande, and S.-H. Han, "Cosensitization effect of  $\text{CdS}/\text{CdSe}$  on the quantum-dots sensitized solar cells," *Electrochim. Acta*, Vol. 50, 2453, 2005.
- [41] W.S. Chen, J.M. Stewart, R.A. Mickelsen, *Appl. Phys. Lett.* 46 (1985) 1095.
- [42] C. Nascu, I. Pop, V. Ionscu, E. Indra, I. Bratu, *Mater. Lett.* 32 (1997) 73.
- [43] H. Okimura, T. Matsumae, R. Makabe, *Thin Solid Films* 71 (1980) 53.
- [44] M.A. Korzhuev, *Phys. Solid State* 40 (1998) 217.
- [45] ASTM Data File Nos. 7-106, 22-252 and 7-110.
- [46] S.J. Fonash, in: *Solar Cells Device Physics*, Academic Press, San Diego, 1981, p. 78.
- [47] R.R. Ahire, B.R. Sankapal, C.D. Lokhande, *Mater. Res. Bull.* 36 (2001) 199.

- 
- [48] C.D. Lokhande, B.R. Sankapal, R.S. Mane, H.M. Pathan, M. Muller, M. Giersig, H. Tributsch, V. Ganeshan, *Appl. Surf. Sci.* 187 (2002) 108.
  - [49] C.D. Lokhande, A. Ennaoui, P.S. Patil, M. Giersig, K. Diesner, M. Muller, H. Tributsch, *Thin Solid Films* 340 (1999) 18.
  - [50] A. Pistone, A.S. Arico, P.L. Antonucci, D. Silvestro, V. Antonucci, *Solar Energy Mater. Solar Cells* 53 (1998) 255.
  - [51] S.D. Sartale, C.D. Lokhande, *Mater. Chem. Phys.* 65 (2000) 63.